"FOTON-M" №4 SPACECRAFT RADIATION ENVIRONMENT AS OBSERVED BY THE RD3-B3 RADIOMETER-DOSIMETER IN JULY-SEPTEMBER 2014

Tsvetan Dachev[1], Borislav Tomov[1], Yury Matviichuk[1], Plamen Dimitrov[1], Nikolay Bankov[1], Vyacheslav Shurshakov[2], Olga Ivanova[2], Donat-Peter Häder[3], Gerda Horneck[4]

[1]Space Research and Technology Institute – Bulgarian Academy of Sciences
tdachev@bas.bg, btomov@bas.bg, ymat@bas.bg, pdimitrov1957@abv.bg, ngb43@abv.bg,
[2]Institute of Biomedical problems, Russian Academy of Sciences, Moscow, Russia
shurshakov@inbox.ru, olivette@mail.ru
[3]Neue Str. 9, 91096 Möhrendorf, Germany
donat@dphaeder.de
[4]DLR, Institute of Aerospace Medicine, Köln, Germany
gerda.horneck@dlr.de

Keywords: *Space radiation, Space weather, Dosimetry, Spectrometry*

Abstract: *Space radiation was monitored using the РДЗ-Б3 (in the following we use the Latin transcription RD3-B3) spectrometer-dosimeter on board a recent space flight of the Russian recoverable satellite "Foton-M" № 4. The instrument was mounted inside the satellite in a pressurized volume together with biological objects and samples. The RD3-B3 instrument is a battery operated version of the spare model of the R3D-B3 instrument developed and built for the ESA BIOPAN-6 facility on Foton M3 satellite launched on September 2007 [1]. It is a low mass, small dimension automated device that measures solar radiation in four channels and ionizing radiation in 256 channels of a Liulin-type energy deposition spectrometer [2]. The paper summarizes the results for the Earth radiation environment at the altitude of 252–573 km.*

АНАЛИЗ НА РАДИАЦИОННАТА ОБСТАНОВКА НА СПЪТНИКА "ФОТОН-М" №4 ИЗМЕРЕНА С РАДИОМЕТЪРА-ДОЗИМЕТЪРА РДЗ-БЗ ПРЕЗ ЮЛИ-СЕПТЕМВРИ 2014

Цветан Дачев[1], Борислав Томов[1], Юрий Матвийчук[1], Пламен Димитров[1], Николай Банков[1] Вячеслав Шуршаков[2], Олга Иванова[2], Донат Хедар[3], Герда Хорнек[4]

[1]Институт за космически изследвания и технологии – Българска академия на науките
tdachev@bas.bg, btomov@bas.bg, ymat@bas.bg, pdimitrov1957@abv.bg, ngb43@abv.bg
[2]Институт за медико-биологически науки, Руска академия на науките, Москва, Русия
shurshakov@inbox.ru, olivette@mail.ru
[3]Neue Str. 9, 91096 Möhrendorf, Germany
donat@dphaeder.de
[4]DLR, Институт по авиационна медицина, Кьолн, Германия
gerda.horneck@dlr.de

Ключови думи: *Космическа радиация, Космическо време, Дозиметрия, Спектрометрия*

Резюме: *Космическата радиация е наблюдавана с помощта на спектрометъра-дозиметъра РДЗ-БЗ (латинската транскрипция е RD3-B3) на борда на руския спътник "Фотон-М" № 4. Инструментът е монтиран в херметичния отсек на спътника заедно с биологични обекти и проби. Инструментът RD3-B3 е, работеща на батерии версия на резервния модел на инструмента за R3D-B3, разработен и изработен за платформата на ESA BIOPAN-6. Същият е летял на спътника Фотон М3 през м. септември 2007 г. и на спътника „БИОН-М" № 1 през м. септември 2013 г. RD3-B3 е автоматизирано устройство с малка маса и малък размер, което измерва слънчевата радиация в четири канала и йонизиращото лъчение в 256 канала в спектрометър с 1 детектор от типа „Люлин". Статията обобщава резултатите за радиационната обстановка на Земята на височина от 252–573 km.*

1. Introduction

"Foton-M" №4 was a Low Earth Orbit (LEO) satellite that orbited the Earth with a period of 89.9 min, an inclination of 65°, and with an initial altitude above the Earth surface in the range 260–574 km, which because of the drag in the neutral atmosphere slowly degraded to altitude range 252–542 km in the last days of the mission.

This paper analyses the results for the radiation environment inside the "Foton-M" №4 spacecraft generated by different radiation sources, including: Galactic Cosmic Rays (GCRs), Inner Radiation Belt (IRB) trapped protons in the region of the South Atlantic Anomaly (SAA) and Outer Radiation Belt (ORB) relativistic electrons. The satellite was launched on 18 July 2014 at 20:50 UTC from the Cosmodrome of Baikonur (Kazakhstan). On 1 September at 9:18 UTC the landing module of "Foton-M" № 4 spacecraft successfully touched down at the Orenburg region, after 45 days in orbit.

There are three principal sources of primary ionizing radiation inside the "Foton-M" №4 spacecraft: (1) Galactic cosmic rays; (2) Energetic electrons and protons are trapped in the geomagnetic field and make up the Earth's radiation belts and (3) Solar energetic particles are high fluxes of charged particles encountered during rare but intense solar flares and coronal mass ejections. Also there exist secondary radiation produced in the shielding materials of the spacecraft and biological objects. Dose characteristics in "Foton-M" №4 spacecraft also depend on many other variables such as the spacecraft orbit parameters, solar cycle phase and current helio-and geophysical activity.

1.1. Galactic cosmic rays

The dominant radiation component in the "Foton-M" №4 radiation environment consists of GCR modulated by the altitude and geomagnetic coordinates of the spacecraft. GCR are charged particles that originate mostly from our Galaxy, the "Milky way". Being accelerated at high energetic sources such as neutron stars and supernovae, GCR are the most penetrating of the 3 major types of primary ionizing radiation [3]. The fluxes and spectra of GCR particles show modulation that is anti-correlated with solar activity. The distribution of GCRs is believed to be isotropic throughout the interstellar space. The energies of GCR particles range from several tens up to 10^{12} MeV nucleon^{-1}. The GCR spectrum consists of 98% protons and heavier ions (baryon component) and 2% electrons and positrons (lepton component). The baryon component is composed of 87% protons, 12% helium ions (alpha particles) and 1% heavy ions [3]. Up to 1 GeV the flux and spectra of GCR particles are strongly influenced by the solar activity and hence show modulations that are anti-correlated with solar activity.

The biological impact of space radiation to humans depends strongly on the particle's linear energy transfer (LET) and is dominated by high LET radiation. Especially important is the effect of the high energy heavy ion component of GCRs (typically referred to as high Z and energy (HZE) particles). Consequently, HZE particles possess high LET and are highly penetrating in the human body, which provides them with a large potential for radiobiological damage [4-6]. The deep and prolonged minimum of the descent phase of solar cycle 23 produced a high flux level of GCR, including a flux of iron ions nearly 20% higher than that observed in the previous solar minima [7].

The daily average GCR absorbed dose rates measured with the R3DE instrument [8] outside of the ISS at about 360 km altitude vary in the range 77-102 μGy day^{-1} with an average of 91 μGy day^{-1}. The measured daily average "Foton-M" №4 GCR dose rates were higher because of the higher altitude and inclination of the spacecraft.

1.2. Trapped radiation belts

Other components of the incident radiation field at "Foton-M" №4 orbit are the trapped protons and electrons of Earth's radiation belts [9]. The trapped protons of the inner radiation belt (IRB) have energies up to several hundreds of MeV and are located between about 1.1 to 2 Earth radii above the magnetic equator. The trapped protons are encountered by "Foton-M" №4 in the region of the South Atlantic Anomaly (SAA) where IRB comes closer to the Earth's surface due to a displacement of the magnetic dipole axes from the Earth's center.

The value of the daily SAA dose rate inside the Russian segment of the ISS measured with an unshielded detector (No 4) of the DB-8 system in the period March-June 2009 [35]; see slide No 15) is estimated to be about 105 μGy d^{-1}. The daily average SAA absorbed dose rates measured with the R3DE instrument [8] outside of the ISS at about 360 km altitude vary in the range 110–685 μGy day^{-1} with an average of 426 μGy day^{-1}. The maximum hourly SAA absorbed dose rates reached 1500–1600 μGy h^{-1}. It was found [10] that the docking of the 78-ton body of US Space Shuttle with the ISS strongly decreases the SAA doses. This is explained by the additional shielding, that the Space Shuttle provides, against the IRB protons. The measured "Foton-M" №4 IRB daily average dose rates are higher because of the higher altitude of the spacecraft and because the smaller effective

aluminum shielding, which is estimated to be about 5 g cm^{-2}. The shielding of the Russian segment of the ISS is higher (~10 g cm^{-2}).

The outer radiation belt (ORB) starts from about four Earth radii and extends to about nine to ten Earth radii in the direction opposite to the sun. The outer belt mostly consists of electrons whose energy is not larger than ~10 MeV. At high latitudes, respectively high L values [11], where the "Foton-M" №4 spacecraft reached the "horns" of the ORB, the dose rates are enhanced by relativistic electrons trapped in the ORB. Relativistic electron enhancements in the ORB are one of the major manifestations of space weather near Earth's orbit. These enhancements occur mainly after magnetic storms. The electron flux may cause problems for components located outside a spacecraft (e.g., solar cell degradation).

The average daily ORB dose rate measured with the R3DE instrument at less than 0.6 g cm^{-2} shielding [8], outside of the ISS at about 360 km altitude is 8.64 μGy day^{-1}, and ranges between 0.25 and 212 μGy day^{-1}. Rare sporadic fluxes of relativistic electrons were measured with the R3DR2 instrument to deliver absorbed doses as high as 3,000 μGy day^{-1} [12]. The measured "Foton-M" №4 average daily dose rates inside the ORB are lower because of the higher shielding of the RD3-R3 instrument inside the "Foton-M" №4 capsule.

1.3. Solar energetic particles (SEP)

A sporadic radiation component in the "Foton-M" №4 orbit is the SEPs. They consist of protons, electrons, helium ions, and HZE ions with energy ranging from a few tens of keV to GeV and the intensity can reach hundreds of particles per cm^{-2} s^{-1} sr^{-1}. It is now widely agreed that SEPs come from two different sources with different acceleration mechanisms working: solar flares themselves release impulsive short-duration events while the coronal mass ejection (CME) shocks produce gradual events [13]. The most intense long-duration SEP events, also with the highest energies, are produced by CME-driven shocks [14]. Electrons with energies of ~0.5 to 1 MeV arrive at the Earth, usually traveling along interplanetary field lines, within tens of minutes to tens of hours. Protons with energies of 20–80 MeV arrive within a few to ~10 h, although some high energy protons can arrive in as early as 20 min. Lantos (1993) in [15] underlined that SEP events are relatively rare and occur most often during the solar maximum phase of the 11-year solar cycle.

2. Instrumentation

In order to determine and quantify the radiation field outside the Foton M2/M3 satellite a radiation environment spectrometer-dosimeters R3D-B2/B3 was developed through collaboration of the Bulgarian and German teams and integrated into the Biopan-5/6 facilities [1, 16]. Both of them worked successfully during the Foton M2/M3 missions. The RD3-B3 spectrometer-dosimeter used at the "Foton-M" №4 mission is a battery operated version of the spare model of the R3D-B3 instrument developed and built for the ESA Biopan-6 facility on Foton M3 satellite in September 2007 [17, 18].

Fig. 1a. RADIUS-MD instrument external view

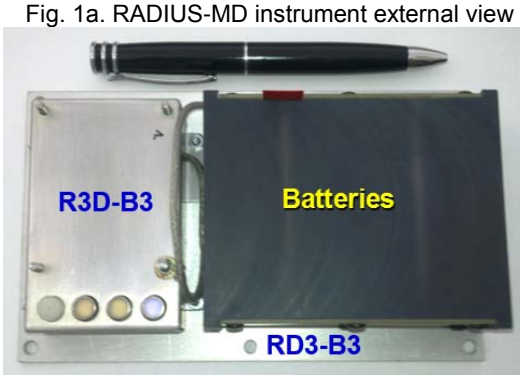

Fig. 1b. External view of R3DE instrument

The scientific objectives of the RD3-B3 spectrometer-dosimeter were in first order connected with the quantification of the global distribution of the radiation field inside the "Foton-M" №4 satellite. Another 22 scientific instruments were also housed inside the satellite related to different scientific disciplines. For many of the experiments on board the knowledge of the space radiation properties is highly important for the interpretation of the data collected during the mission.

The RD3-B3 instrument is a Liulin-type single detector instrument which were successfully flown: 1) In ISS in May-August 1991 [19-22]; 2) Outside ESA Biopan 5/6 facilities on Foton M2/M3 satellites in 2005/2007 [16, 18]; 3) Inside the ESA EXPOSE-E/R/R2 facilities outside ISS in 2008–2010 [8, 12, 23]. Very similar to the "Foton-M" № 4 experiment, using the same RD3-B3 spectrometer-dosimeter, was performed between 18 July and 1 September 2014 in the "BION-M" № 1 spacecraft [24].

Fig. 1a presents the RD3-B3 instrument as situated inside the “Foton-M” №4 capsule, while Fig. 1b gives the external view. On the right side of the Fig 1b the two Lithium-ion battery housing are seen, while on the left side there is the R3D-B3 instrument. The RD3-B3 instrument is a low mass, small dimension automatic device that measures solar radiation in four channels and ionizing radiation in 256 channels of a Liulin-type energy deposition spectrometer. The four solar UV and visible radiation photodiodes are seen as small cylinders on the surface of the R3D-B3 instrument in the right part of Fig. 1b. They were active during the flight of the “Foton-M” №4 satellite but because of the darkness inside the capsule the obtained values were equal to zero. The ionizing radiation detector is situated behind the aluminum wall of the instrument and is not seen on the figure. The aluminum box of R3D-B3 instruments has a size of 53x82x28 mm and 120 g weight.

The cosmic radiation is determined using a semiconductor detector (2 cm^2 area and 0.3 mm thick). After passing through a charge-sensitive preamplifier the signal is digitized (12 bit A/D). A pulse height analysis technique is used to measure the deposited energies (doses) in the detector. Charge pulses generated in the detector are preamplified and then passed to the discriminator. The amplitudes of the pulses are detected and converted into digital signals, which are subsequently sorted into 256 channels according to their amplitudes by a multi-channel analyzer. One energy deposition spectrum is accumulated over 60 s. The highest energy channel stores all pulses with amplitudes higher than the sensitivity range (19.5 mV–5.0 V) of the detector, which response to the energy deposition range (0.081-20.83 MeV). Incoming space radiation sources are characterized using the methods described by Dachev (2009) in [28].

The RD3-R3 instrument is a Liulin-type instrument. These instruments were calibrated in a wide range of radiation fields. First, they were irradiated in gamma and neutron (^{137}Cs, ^{60}Co, AmBe and ^{252}Cf) isotope source radiation fields and at the CERN-EC high energy reference field [25, 26]. The calibrations revealed that except for charged energetic particles, the detector has a high effectiveness for detecting gamma rays. The detectors’ neutron effectiveness depends on the energy of the neutrons. The absolute dosimetric calibrations with a standard ^{137}Cs gamma source give better than 10% accuracy of the dose rate measured by a Liulin spectrometer [26].

Next, the spectrometers were calibrated at the cyclotron at Universite Catholique de Louvain, Louvain-la-Neuve, Belgium [26], and by using proton and heavy ion beams from the NIRS Cyclotron facility and the HIMAC heavy ion synchrotron facility at NIRS, Chiba, Japan [27]. All calibration results and also the GEANT-4 and PHITS code simulations revealed very good coincidence between measured and predicted energy depositions spectra and proved the effectiveness of the Liulin spectrometers for the purposes of characterization of the space radiation field [28].

The total external shielding in front of the detector of the RD3-B3 instrument is not well known but very rough estimations give values between 2 and 70 g cm^{-2} aluminum material for different angles of view of the instrument, with a minimal value toward the wall of the capsule (see Figure 1) and maximal value toward the internal instrumentation package of the capsule. The calculated stopping energy of normally incident particles to the detector of the instrument behind 2 g cm^{-2} aluminum material is 3.25 MeV for electrons and 41 MeV for protons [29]. This means that only protons and electrons with energies higher than those mentioned above could reach the detector of the RD3-B3 instrument. The instrument registered bremsstrahlung radiation from the electrons impacting the walls of the “Foton-M” №4 capsule but this source is not possible to be distinguished from the primary electron flux because both sources delivered similar small specific doses.

3. Data analysis and results

3.1. All data presentation

“Foton-M” №4 mission took place in the declining phase of the 24th solar cycle, and the satellite flew during a period characterized by moderate solar activity. One relatively small SEP event were measured by GOES 13 satellite, which maximum occurred about midday on 25 August 2014. No real enhancement in the proton flux with energies above 100 MeV was observed in the GOES-13 data. That is why the R3D-B3 instrument being behind thick shielding was not able to register it.

The geomagnetic field during the “Foton-M” №4 flight was also at a moderate level with a 3 small magnetic storms on 6, 21 and 27 August. The last one is the most powerful and the Dst index reaches of about -90 nT.

The absorbed doses and satellite altitude during the whole space monitoring period in the Silicon detector of the RD3-B3 instrument (18 August to 1 September 2014) are plotted in Fig. 2. The red points against the left side axis in the upper part of the figure correspond to the dose rates in μGy h^{-1}. The satellite altitude variations are presented only with the linear approximation, plotted with blue line against the right side axis and showing the average altitude degrade from about 410 km down to 400 km above the Earth surface at the end of the mission.

The recorded maxima in the upper part of Fig. 2 were obtained during the crossings of the maxima of IRB in the SAA region where the inner radiation belt populated with high-energy protons is encountered. More detailed look on the maximal IRB dose rates shows that they degraded from about 3500 11 μGy h^{-1} down to 2200 μGy h^{-1}.

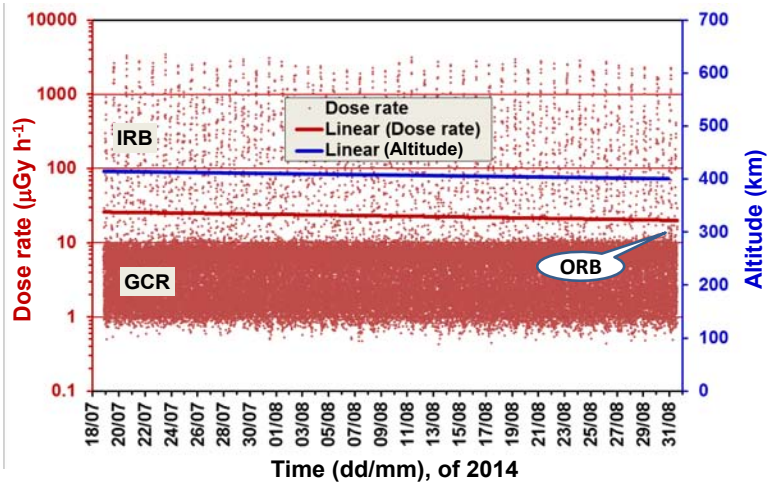

Fig. 2. Absorbed dose rate and altitude variations during the whole in space monitoring period of the RD3-B3 instrument (18 July to 1 September 2014)

The area with dose rates between 0.5 and 10-11 μGy h^{-1} is generated by the variations of GCR values when the satellite crosses the geomagnetic equator (~0.5 μGy h^{-1}) and returns back to high latitudes in the polar regions (~11 μGy h^{-1}). Few small maxima In the lower right angle of the figure up to about 22 μGy h^{-1} is generated after the magnetic storm on 26 August relativistic electrons in the other radiation belt [30].

The total (GCR+IRB+ORB) absorbed dose rates were presented by linear approximation seen with red line in the range 27-20 μGy h^{-1}. The comparison of the slope of linear approximation of the absorbed dose rate with altitude linear approximation slope reveal the conclusion that the dose rate degradation is due to the satellite altitude degradation. Keeping in mind that the GCR dose rates seen in Fig. 2 don't show any altitudinal dependence and that the ORB input in the total dose rate is negligible. The main contribution to the altitudinal effect is from the IRB variations.

3.2. Analysis of the recorded space radiation sources

During the analysis of the data from ISS a selection procedure was established to distinguish between the three expected radiation sources: (i) GCR particles, (ii) protons in the SAA region of the IRB and (iii) relativistic electrons in the ORB [28, 31]; It was shown that the dose to flux ratio or specific dose (SD) can characterize the type of the predominant radiation source in Liulin-type instruments in the near-Earth radiation field. The SAA and ORB data, which have relatively high fluxes, can be split into two parts by the simple relation of the SD. This split is based on the fact that one IRB proton with an energy in the range of few tens to a few hundred MeV can deposit between 6.5 and 1.12 nGy cm^2 $part^{-1}$ in the detector, whereas one outer radiation belt relativistic electron with an energy in the range 1–10 MeV because of the much smaller mass, can only deposit between 0.3 and 0.35 nGy cm^2 $part^{-1}$. GCR protons in equatorial and low latitude regions have very small fluxes of less than 1 particle cm^{-2} s^{-1}, which is why the dose rate to flux ratio (D/F) is not stable and varies in the range from 0.03 to 30 nGy cm^2 $part^{-1}$ (please refer to Figure 5 of Dachev et al., 2012b). This variation makes the SD inapplicable for characterization of the GCR radiation source.

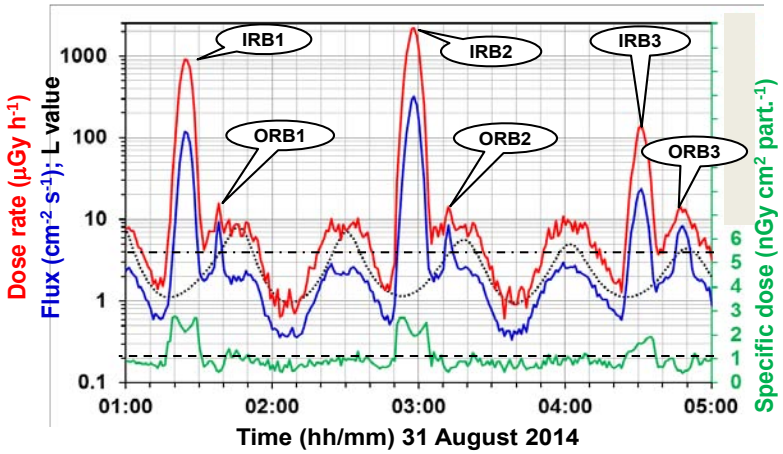

Fig. 3. Presentation of the RD3-R3 data along the orbit of the satellite with higher resolution than on Figure 2

Figure 3 presents, with better resolution than Figure 2, the measured data at 6 UT hours along the orbit of the satellite on 31 August 2014. Dose rate in μGy h^{-1}, flux in cm^{-2} s^{-1} and the McIlwain parameter L (dotted curve) are plotted with different colors against the left Y axes. The calculated SD in nGy cm^2 $part^{-1}$ [28, 31] are plotted with green curve against the right Y axes. The dashed horizontal line at SD=1 nGy cm^2 $part^{-1}$ and the dot-dashed horizontal line at L=4 are plotted also to help with better understanding of the figure.

The observations start at the left side of the figure with part of descending orbit, which first crosses the magnetic equator and then goes through the Eastern part of the SAA region seen as a maxima of the flux and dose rate (IRB1) and -as a maximum of the SD value. Further the satellite reaches higher latitudes in the Southern hemisphere at L value of about 4 which is seen as a maxima of dose rate and flux. In the same place a well seen minimum of the SD value below 1 nGy cm^2 $part^{-1}$ is observed; the SD value confirms that the maximum (ORB1) is populated by energetic electrons. Further the satellite crosses the highest L value of about 8 and returns to the equator. The crossing of northern hemisphere L values about 4 around 02:30 UTC is connected with two small maxima in the dose rate and flux. The lack of well seen minimum in the SD below 1 nGy cm^2 $part^{-1}$ brings controversial information and we are not able to conclude that these are ORB maxima. In the next part of Figure 3 the described sequence of the satellite movements is repeated 1.5 times. Each next crossing of the equator is shifted with 15° to the West that is why the middle maximum seen in the figure crosses close to the central part of the SAA.

More precisely the observed peculiarities of the space radiation can be described as follows:

1) There are three passes across the SAA region, which are seen as large maxima in the dose rates reaching values of 900, 2100 and 150 μGy h^{-1} from left to right. Flux values in these maxima are also high and reach 110, 300 and 24 cm^{-2} s^{-1}. The SD values in all three cases are larger than 1 nGy cm^2 $part^{-1}$.

2) Five maxima corresponding to passes across the high latitude GCR regions in both hemispheres are well seen in the dose rate curve in Fig 3. The flux curve presented with a blue line forms three prominent maxima at L values around 4. The dose rate curve in the L~4 region corresponds to the flux maxima but with smaller amplitudes. These maximums have to be attributed to the crossings of the Southern outer radiation belts regions where relativistic electron fluxes are observed (Zheng et al., 2006; Wrenn, 2009; Dachev et al., 2009 and 2012ab). In the L~4 regions the RD3-R3 instrument registered bremsstrahlung radiation from the energetic electrons impacting the walls of the capsule but this source cannot be distinguished from the primary electron flux because both sources deliver similar small specific doses. The SD values inside the three flux maxima at L~4 are less than 1 nGy cm^2 $part^{-1}$ and confirm the expectations made by Heffner (1971) and Dachev (2009)
[28, 31].

3) There are also five passes across the magnetic equator, where deep dose rate minima around 1 μGy h^{-1} are observed. The flux values are around 0.3-0.4 cm^{-2} s^{-1}.

Figure 4 summarizes all RD3-B3 data to analyze the peculiarities of the space radiation sources. The abscissa plots the measured fluxes in cm^{-2} s^{-1}, while the ordinate shows the dose rate in μGy h^{-1} and SD in nGy cm^2 $part^{-1}$ for the period 18 July-1 September 2014. The large amount of points in the diagonal of the figure (please see the ovals labeled with "GCR", "Inner belt protons" and "Outer belt electrons") is responsible for the dose rate values, which, as expected, are in linear dependence from the flux, while the almost horizontally plotted blue points present the SD values.

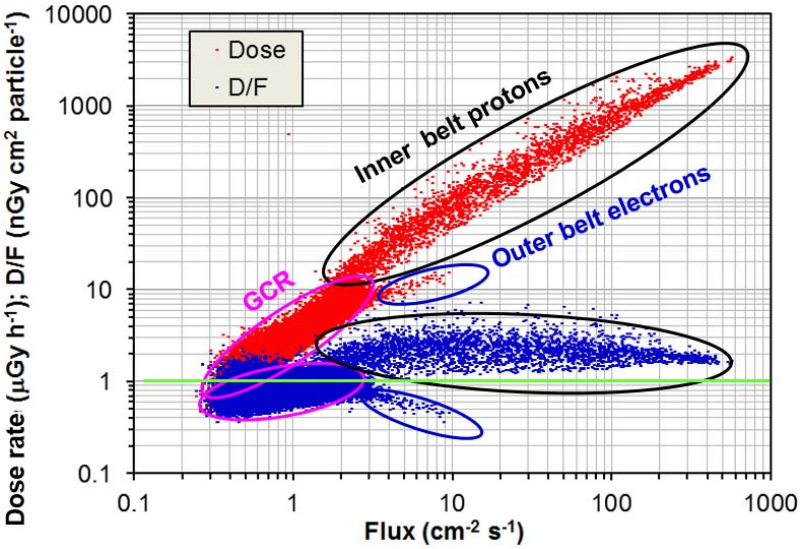

Fig. 4. Characterization of the RD3-B3 predominant radiation sources by the dose rate from flux and specific dose dependencies

Three branches in each graphic are differentiated in Figure 4. The highly populated part in the diagonal array of points: 1) shows a large amount in the range 0.3–15 μGy h^{-1}; (2) for a fixed flux a wide range of doses is observed. These two features could be explained only by the GCR particles, which, being of small statistical relevance and high LET, are able to deposit various doses for a fixed flux value. The smallest dose rates (0.3–0.4 μGy h^{-1}) are observed close to the magnetic equator, while the largest are at high latitudes. In the horizontal graphic this part of the data is represented with a similar large amount of points, which on a large scale they overlap the dose rate points in the diagonal. They are distributed on both sides of the solid horizontal (green) line representing the SD value of 1 nGy cm^2 $part^{-1}$, with a small trend toward higher SD values when the dose rate increases.

The amount of points in the diagonal graphics within the dose rate range 9–18 μGy h^{-1}, represented in the horizontal graphic with points, which extend up to 10 cm^{-2} s^{-1} are with SD values below 1 nGy cm^2 $part^{-1}$ (the (green) horizontal line). This amount of points is based on low LET particles and could be formed only by the relativistic electrons or bremsstrahlung [28] in the outer radiation belt. Here, because of higher shielding (more than 5 g cm^{-2} aluminum), the relativistic electrons fluxes and dose rates measured with the RD3-R3 instrument are much lower than those presented in the above referenced papers.

The amount of points in the diagonal graphics within the dose rate range 20–3300 μGy h^{-1} has a different source compared to the previous two. This amount of points could be formed only by protons from the IRB (The region of the South Atlantic Anomaly (SAA)) whose dose depositions depend on the energy. The smaller energy protons are depositing higher doses. In the horizontal direction, the graphic of these points has a similar form and is situated in the range 1.2–8.5 nGy cm^2 $part^{-1}$. Both IRB and ORB amount of points can be approximated by straight lines. From these approximations we conclude that 1 proton in IRB produces a dose of 1.4 nGy on average in the silicon detector, while 1 electron in ORB produces a dose of 0.33 nGy, which is in good agreement with Heffner's formulas [31].

The black text in Table 1 summarizes the observations during "BION-M" No. 1 mission, while the red text presented the "Foton-M" №4 spacecraft data. In the last 2 columns of Table 1 the selecting requirements are presented. The number of measurements, the hourly and daily average

Table1. The black text in Table 1 summarizes the observations during "BION-M" No. 1 mission, while the red text presented the "Foton-M" №4 spacecraft data

Source	Number of Meas./ Days [No]/ [Days]	Aver. Dose Rate/ Aver. Flux/ Aver. daily dose [μGy h^{-1}]/ [cm^{-2} s^{-1}]/ [μGy day^{-1}]	Min. Dose Rate/Min. Flux/Min. daily dose [μGy h^{-1}]/ [cm^{-2} s^{-1}]/ [μGy day^{-1}]	Max. Dose Rate/Max. Flux/Max. daily dose [μGy h^{-1}] / [cm^{-2} s^{-1}]/ [μGy day^{-1}]	Total Dose Rate/Fluen. [mGy]/ [No of events/particles]	Aver. Altitude [km]	Aver. Lat./L [Deg.]/L Value	Aver. Long. [Deg.]	Selecting requirements	
									Dose Rate/Flux [μGy h^{-1}]/ [cm^{-2} s^{-1}]	SD/B [nGy cm^2 $part^{-1}$]/ [Gauss]
All data	34391/ 64108 23.883/ 44.52	41.03/22.8 6.05/3.76 985/546	0.4/0.42 0.26/0.24 495/436	4530/3413 700/563 1139/662	23.52/ 24.35 4,159,420/ 4,815,080	561/407	-0.06/-1.12 3.0/	0.08/ 0.013	No	No
GCR	28977/ 60997 20.123/4 2.36	5.1/4.4 1.47/1.32 102.8/100.6	0.4/0.42 0.26/0.24 93.6/97.3	14.8/15 10.12/2.9 111.6/105.3	2.366/4.47 850,045/ 1,611,340	559/400	3.5/1.6 3.1/3.1	5.5/3.7	Flux<2.9	B>0.23/ Dose<15
IRB (SAA)	1762/ 2705 1.228/ 1.88	700/439 88.7/59 908/443	20.04/20.02 1.63/1.96 815/330	4530/3413 700/563 1017/562	20.57/19.7 3,125,640/ 3,133,000	565/497	-24.9/ -28.2 1.39/1.5	-44.6/ -43.12	Dose>20	SD>1.12
ORB	462/96 0.32/ 0.066	11.2/9.93 5.33/4.79 4.2/ 0.018	6.7/6.2 2.9/2.9 0.0/0.0	22.61/15.66 14.53/9.36 10.4/0.54	0.087/0.019 49,220/ 14,400	581/491	-22.5/ -45.2 4.08/ 4.15	11.3/ 12.7	Flux>2.9	SD<0.7

and total accumulated dose rates and fluencies are calculated and presented for all data and for each of the three major sources. The averaged coordinates: longitude, latitude, L value and altitude where the averaged values are obtained and also presented in 3 columns. The presented values in the "All data" row of the table cover all data in the period 18/07/2014 - 01/09/2014.

GCR data were selected using three requirements: 1) The flux values to be less than 2.9 cm^{-2} s^{-1}, which cuts the high flux level in the ORB (cf. Figure 4); 2) The total magnetic field strength to be greater than 0.23 Gauss, which cuts the data obtained inside the SAA region; 3) The dose rate to be less than 15 μGy h^{-1}. The average daily value was obtained by averaging all observed GCR single measurements for each full day.

The IRB (SAA) data in Table 1 were selected by two requirements. The first is that the dose rate values to be higher than 20 μGy h^{-1}. This cuts the GCR dose rates, which usually deposited smaller values. The second requirement is the SD value to be higher than 1.12 nGy cm^2 $part^{-1}$. According to Heffner's formulas (Heffner, 1971) this selects only depositions by protons excluding relativistic electrons and/or bremsstrahlung dose rates higher than 20 μGy h^{-1}. The values presented in Table 1 for "BION-M" No. 1 mission cover the circular orbit data from 22 April to 12 May 2013. The average daily values were obtained by averaging all observed IRB single measurements for each full day.

The ORB data in Table 1 were selected by: 1) The flux values to be higher than 2.9 cm^{-2} s^{-1}, which cuts the low flux level in the GCR; 2) SD value to be less than 0.7 nGy cm^2 $part^{-1}$. This according to Heffner's formulas [31] selects only depositions by relativistic electrons and/or bremsstrahlung excluding proton depositions from GCR or IRB. The average daily values were obtained by averaging all observed ORB single measurements for each full day.

3.3. – Comparison of the "BION-M" No. 1 and "Foton-M" №4 data

The comparison of the values obtained with the RD3-R3 instrument on spacecraft with the values on "BION-M" No. 1 mission and analog values obtained at the International space station (ISS) reveal the following results:

1) The total dose of 24.36 mGy obtained at the "Foton-M" №4 satellite is almost the same as that observed on "BION-M" No. 1 of 23.52 mGy, nevertheless the total amount of days at the "Foton-M" №4 satellite of 44.52 days is close to 2 times larger than on "BION-M" No. 1 (23.883 days). The main reason is that "Foton-M" №4 satellite spent all the time on elliptical orbit with average altitude of 407 km, which accumulates less IRB doses than the circular orbit at 561 km of "BION-M" No. 1 satellite.

2) The GCR average daily dose rate of 100.6 μGy day^{-1} obtained at the "Foton-M" №4 satellite is almost the same as that observed on "BION-M" No. 1 and higher than that measured at the ISS [8] of 91.1 μGy day^{-1} because the "Foton-M" №4 altitude and inclination of the orbit are higher than the respective ISS parameters (360 km altitude and 51.6° inclination). In addition, the ISS data are obtained behind less shielding (0.45 g cm^{-2}) than those on "Foton-M" №4 satellite.

3) The IRB average daily dose rate of 443 μGy day^{-1} obtained at the "Foton-M" №4 satellite is smaller than observed on "BION-M" No. 1 (908 μGy d^{-1}), mainly because smaller average altitude of the IRB measurements (565 km on "BION" and 497 km on "Foton"). In same time both values are higher than that measured in the ISS. The value of the daily SAA dose rate inside the Russian segment of the ISS, measured with an unshielded detector (No 4) of the DB-8 system in the period March-June 2009 (Benghin et al., 2010; see slide No 15) is estimated to be about 105 μGy d^{-1}, which is much less than the averaged values obtained by us on the "Foton-M" №4 where the dose rate is more than 4 times higher reaching 443 μGy day^{-1}. Gaza et al. (2010) [36] presented the whole dynamics of the daily dose rate dependence on the location in the station. Their slide No 5 shows that the total daily dose rate (GCR+SAA) measured by 22 passive dosimeters (ISS Radiation Area Monitors) vary from about 160 μGy d^{-1} in the well-shielded locations up to 360 μGy d^{-1} in the less shielded locations.

4) As already mentioned, the outer radiation belt relativistic electron dose rates on "Foton-M" №4 satellite are very small because of large shielding. They are practically not comparable with data obtained outside the ISS. The ORB data were enhanced after 26 August small magnetic storm.

The analysis of the fluence data shows that the whole amount of more than 4.8 million events (particles) in the detector of the RD3-R3 instrument during the flight the "Foton-M" №4 is distributed as follows: a) The largest amount (more than 3 million) of protons was registered in the IRB source, which produces the largest hourly and daily absorbed dose rates. b) The GCR dose was produced by more than 1.6 million events (particles). c) The amount of ORB relativistic electrons and/or bremsstrahlung events is the smallest with of a value a little higher than 14 thousand.

The average specific doses show the following values: All data - 1.008 nGy cm^2 $part^{-1}$; GCR - 0.941 nGy cm^2 $part^{-1}$; IRB - 2.31 nGy cm^2 $part^{-1}$; ORB - 0.61 nGy cm^2 $part^{-1}$. The IRB values correspond well with Heffner's formulas [31]. The ORB average SD value is larger than that expected from Heffner's formulas because the 1-min spectra are mixed by GCR, relativistic electrons and/or bremsstrahlung events. The presence of GCR particles increases the SD value.

3.4. Latitudinal distributions of the data

Figure 5 presents the distribution of the obtained dose and flux data and the calculated SD values in nGy cm^2 $part^{-1}$ against the L value up to 7 [11]. The whole range of L values data is between 0.985 and 34.95. The dose rate, flux and SD values are practically constant above an L value of 7 that is why they are not shown in the graphic.

The dose rate and flux data in Fig. 5 show two obvious maxima – one at L values of about 1.25 and another at about 4. The lower L value maximum corresponds to the inner (proton) radiation belt, which is populated mainly by protons with energies from a few tens to a few hundred MeV. Because of differences in the altitude of the ascending and descending orbits, which will be studied further in the paper, the IRB maximum is divided by 2 maxima: the first one with maximal dose rate of 3412 μGy h^{-1}, at average L=1.2 and average altitude of 523 km is generated during the descending orbits of the satellite; The second one with maximal dose rate of 1525 μGy h^{-1} at average L=1.45 and average altitude of 424 km is generated during the ascending orbits of the satellite

The poor seen maximum at L=4.2 corresponds with the outer (electron) radiation belt, which is populated mainly by electrons with energies from hundreds of keV to a few MeV. As already mentioned, the calculated stopping energy of normally incident particles to the detector of the RD3-R3 instrument is 3.55 MeV for electrons and 41 MeV for protons (Berger et al., 2013). This means that only protons and electrons with energies higher than those mentioned above outside the satellite could reach the detector inside.

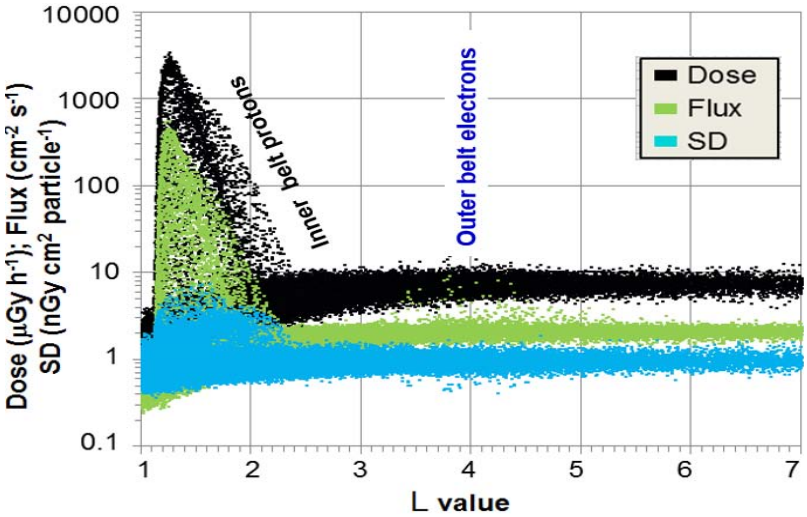

Fig. 5. Distribution of dose and flux and SD data against the L value

The large amount of measurements in Fig. 5 with more than 1000 points per day is concentrated in the zone of GCR, which is seen as an area with many points in L-values between 1 and 7. The covered dose rate range is between 0.3 and 10–15 μGy h^{-1}. The lowest rates are at low L values, close to the magnetic equator, while the highest are at high latitudes equatorward from both magnetic poles. The GCR radiation source has a ''knee" at L value about 3. The large amount of SD points close to 1 nGy cm^2 $part^{-1}$ is produced by GCR, representing high LET particles which are able to delivery different doses with the same flux values. The GCR had very small fluxes and Heffner's formulas are not applicable for them.

The specific dose (SD) value is provisionally divided into two parts – below and above 1 nGy cm^2 $part^{-1}$. This value divides the range of SD delivered by relativistic electrons and/or bremsstrahlung below about 0.6 nGy cm^2 $part^{-1}$ and by protons above 1.12 nGy cm^2 $part^{-1}$.

The amount of flux points with values above 2 cm^{-2} s^{-1} in the region of L values 3-5 is visually larger than the corresponding amount of dose rate points. This is because the doses delivered by relativistic electrons and/or bremsstrahlung are very small and their contribution in the predominated by GCR deposited energy spectra is practically not seen.

Generally, the radiation sources and SD variations on the "Foton-M" №4 satellite are with small dynamics in comparison with analog distributions obtained on Foton-M2/M3 satellites and on the ISS with instruments outside the pressurized volume.

3.5. Daily average data

Fig. 6 presents the time variations of the daily averaged data for the different radiation sources on Foton-M No4 satellite. On the vertical axes is the daily average dose rate in μGy day^{-1} and the daily averaged altitude, while on the horizontal axes is the UTC time from 19 July to 2 September 2014.

The total daily, IRB daily and GCR daily are presented with continues curves. The ORB daily being sporadic is presented with single points, which maximum is in the data after the magnetic storm on 26th August 2014. The GCR daily values are also affected by the magnetic storm and show clear Forbush decrease [32] after 26th August 2014. The very slow upward trend of the daily GCR dose rates is due to solar modulation, which predict rise of the GCR flux and respectively dose rate when the solar activity fall down.

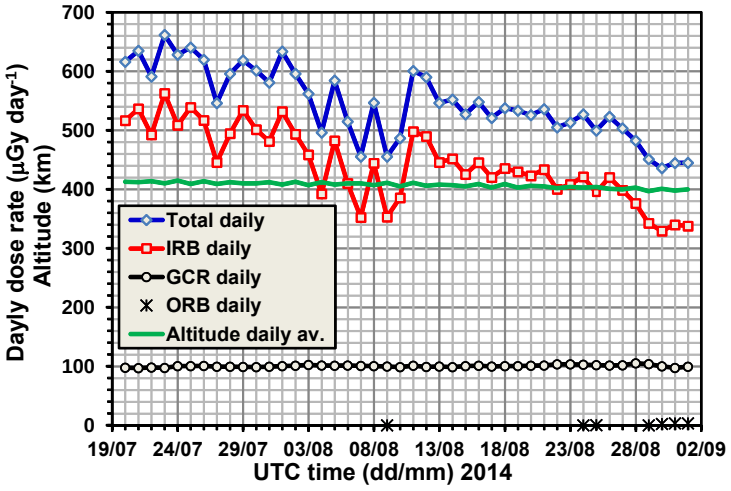

Fig. 6. Daily average data for the different radiation sources on Foton-M No4 satellite

Most affected by the relative small daily average altitude decrease from about 412 km down to 400 km are the IRB daily dose rates, which fall from about 600 μGy day^{-1} down to 340 μGy day^{-1}. The

"Foton-M №4" satellite measurements is performed at the bottom side of the IRB altitudinal profile where the dependence of the flux rate and dose rate respectively is in exponential low function from the altitude. The altitudinal dependence in the bottom part of the IRB is a well-known phenomenon which has been competently described elsewhere [33, 34]. Therefore, it will not be discussed further.

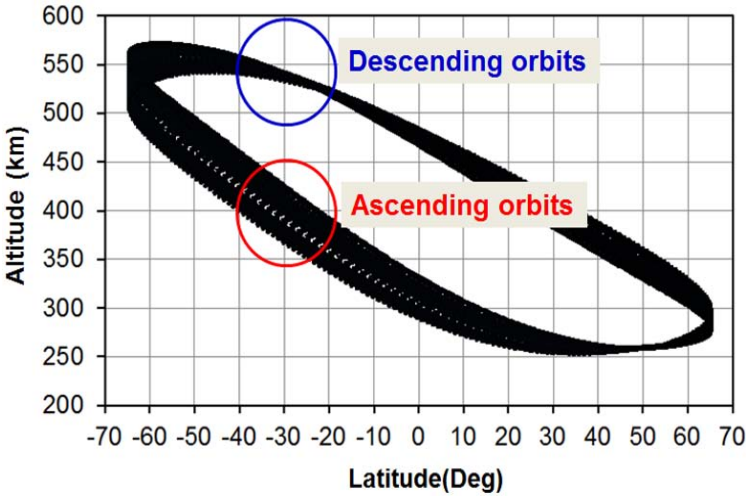

Fig. 7. The altitude of the descending orbits crossings of the expected places of the SAA maximum is more than 100 km higher than the ascending

3.6. Ascending/descending orbit dependence

Fig.7 presents the whole time evaluation of the "Foton-M №4" satellite altitude. It is seen that the altitude of the descending orbits crossings of the expected places of the SAA maximum is more than 100 km higher than the ascending. This implement strong altitudinal dependence, which influence all kind of space distributions of the data. Example has been already shown in the paragraph 3.3. "Latitudinal distributions of the data". Same is truth for the global distributions, which is studied in next paragraph.

3.7 Global distributions of the data

Figures 8b and 8c present the averaged contour view of the global distribution of the RD3-R3 dose rate data for the descending (Fig. 8a) and ascending (Fig. 8b) orbits of the "Foton-M №4" satellite, which are compared with the predicted ones at an altitude of 573 km by the AP/AE-8 MAX models (http://www.spenvis.oma.be/); Vette, 1991) proton fluxes above 100 MeV and electron fluxes above 5 MeV in Fig. 8a.

In Fig. 8b/c, except the global map of the flux, the isolines of the L value for the 2005 epoch (McIlwain, 1961; Heynderickx et al., 1996) at the altitude of the "Foton-M" №4 satellite are also presented with dashed lines. The exact values of the dashed isolines are for the following L values: 1, 1.2, 1.6, 2, 4, 8 and 16. The L=4 isoline is presented with a heavy line. It is seen that the lines of equal dose rates in the north and south high latitude regions follow very well the L-shell isolines as expected.

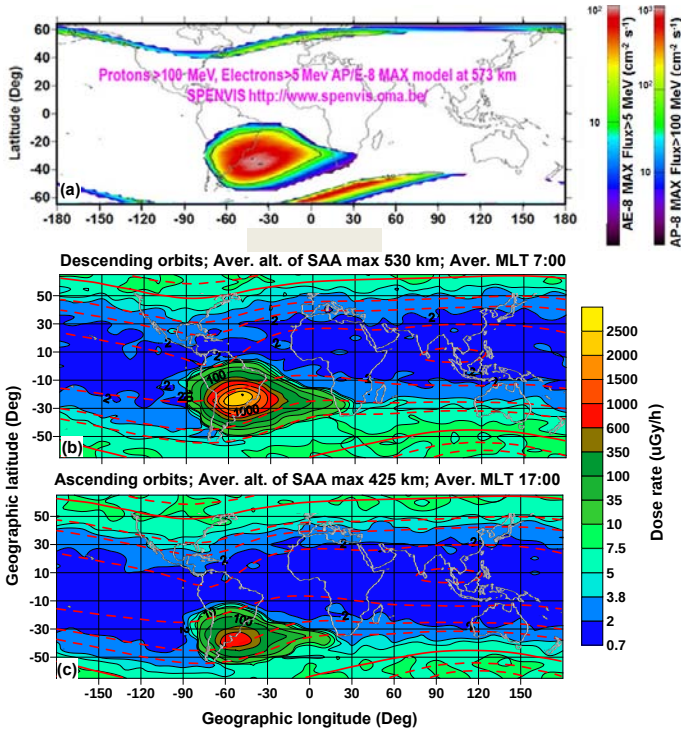

Fig. 8. Figures 8b and 8c present the global distribution of the RD3-R3 dose rate data for descending orbits (8a) and for ascending orbits (8c), which are compared with the predicted ones by the AP-8/AE-8 MAX models proton fluxes above 100 MeV and electron fluxes above 5 MeV in Fig. 8a

In Figure 7b the areas outside the SAA region present the averaged GCR dose rate distribution, forming a wide minimum close to the geomagnetic equator and rise toward the magnetic poles in both hemispheres. The observed almost dose rate maximum close to L=4 shows the position and shape of the ORB, which coincides relatively well with the one predicted by the AE-8 MAX model.

The external oval of the SAA RD3-R3 data in Fig, 8b and the ones predicted by the AP-8 MAX model in Figure 8a are similar, but the position of the maximum of the SAA observed in 2014 is moved to the west in comparison to the model, which is calculated for the epoch of 1970, for the maximum of

the solar activity at altitude of 573 km and for protons with energies larger than 100 MeV. The geographic coordinates of the SAA maximum is influenced by the secular drift of the geomagnetic field (Fraser-Smith, 1987), which leads to a movement of the SAA maximum in the North-West direction. This phenomenon will be more precisely studied in future investigations of the "Foton-M" № 4 data.

4. Conclusions

This paper analyses the results for the radiation environment obtained by the RD3-R3 instrument inside the "Foton-M" №4 spacecraft and generated by different radiation sources, including: galactic cosmic rays (GCRs), inner radiation belt (IRB) trapped protons in the region of the South Atlantic Anomaly (SAA) and outer radiation belt (ORB) relativistic electrons. The satellite was launched on 18 July 2014 at 20:50 UTC from the Cosmodrome of Baikonur (Kazakhstan). On 1 September at 9:18 UTC the landing module of "Foton-M" №4 spacecraft successfully touched down at the Orenburg region, after 45 days in orbit.

The observed hourly and daily IRB dose rates at the "Foton-M" №4 satellite are the highest seen by us during our measurements on "Mir" and the ISS space station and on Foton-M2/M3 satellites because the altitude of the "Foton-M" №4 obit was the highest in comparison with all missions mentioned above. The same is valid for the GCR doses. The observed ORB doses are smaller than the ones measured outside the ISS because of the higher shielding on the "Foton-M" № 4 satellite.

The comparison of the "Foton-M" №4 satellite data with the similar data obtained on "BION-M" No. 1 satellite shows that: 1) The GCR average daily dose rate of 100.6 μGy day^{-1} obtained at the "Foton-M" №4 satellite is almost the same as that observed on "BION-M" No. 1; 2) The IRB average daily dose rate of 443 μGy day^{-1} obtained at the "Foton-M" №4 satellite is smaller than observed on "BION-M" No. 1 (908 μGy d^{-1}), mainly because smaller average altitude of the IRB measurements (565 km on "BION" and 497 km on "Foton"); 3) The total dose of 24.36 mGy obtained at the "Foton-M" №4 satellite is almost the same as that observed on "BION-M" No. 1 of 23.52 mGy, never the less that the total amount of days at the "Foton-M" №4 satellite of 44.52 days is close to 2 times larger than on "BION-M" No. 1 (23.883 days). The main reason is that "Foton-M" №4 satellite spent all the time on elliptical orbit with average altitude of 407 km, which accumulates less IRB doses than the circular orbit at 561 km of "BION-M" No. 1 satellite.

The difference of more than 100 km between the ascending and descending IRB altitudes implement strong altitudinal dependence, which influence all kind of space distributions of the "Foton-M" №4 data. The phenomenon was studied for the L value and global distributions of the dose rate data.

As mentioned above, one of the purposes of the RD3-R3 measurement is to provide information on the diurnal variation of the space radiation to the scientists from other "Foton-M" №4 experiments. The detector of the RD3-R3 instrument was located behind about 5 g cm^{-2} shielding that is why the obtained IRB and ORB dose rate is applicable only for other experiments behind a similar shielding. Experiments located deeper inside the "Foton-M" №4 capsule experience smaller IRB and ORB daily dose rate doses than those shown in Table 1.

The daily average global GCR dose rate is valid for almost all depths and positions of the "Foton-M" №4 experiments. To obtain the total accumulated dose from GCR, it is necessary to multiply the average daily dose rate in Table 1 by the number of exposition days. Some small increase of the GCR doses can be expected behind thicker shielding because additional doses from secondary particles will be generated in the shielding [21] (see Fig. 14).

Despite its very small size and low power consumption the RD3-B3 instrument has been proven to reliably characterize the radiation environment in the "Foton-M" №4 satellite, including the relativistic electron precipitations. This was achieved mainly with the analysis of the deposited energy spectra, obtained at each measurement cycle of 60 s. The obtained daily and hourly values for the space radiation are the input to other experiments on the capsule with a precise history of their accumulation and can contribute to a better understanding of the results from the biological experiments.

5. Acknowledgements

This work is partially supported by the Bulgarian Academy of Sciences, Agreement between BAS and RAS on fundamental space research.

References:

1. Häder, D.-P. and Dachev, T. P. Measurement of solar and cosmic radiation during spaceflight. Kluwer Press, Surveys in Geophysics, 24, 229-246. 2003.

2. Dachev, T. P., J. V. Semkova, B. T. Tomov, Yu. N. Matviichuk, Pl. G. S. Maltchev, R. Koleva, Pl., Dimitrov, N. G. Bankov, V. V., Shurshakov, V. V., Benghin, E. N., Yarmanova, O. A. Ivanova, D.-P. Häder, M. T. Schuster, G. Reitz, G. Horneck, Y. Uchihori, H. Kitamura, O. Ploc, J. Kubancak, I. Nikolaev. Overview of the Liulin type instruments for space radiation measurement and their scientific results, 92–114, 2015, http://dx.doi.org/10.1016/j.lssr.2015.01.005.
3. Simpson, J. A . in: Shapiro M.M. (Ed.) Composition and origin of cosmic rays, NATO ASI Series C: Mathematical and Physical Sciences. Vol. 107, Reidel, Dordrecht, 1983.
4. Kim, M.-H.Y., Angelis, G. De., Cucinotta, F. A. Probabilistic assessment of radiation risk for astronauts in space missions. Acta Astronaut. 68 (7–8), 747–759. April–May 2011, 2010.
5. Benton E. R. and Benton E. V. Space radiation dosimetry in low-Earth orbit and beyond, Nucl. Instrum. and Methods in Physics Research, B, 184, (1-2), 255-294, 2001.
6. Horneck, G. HZE particle effects in space. Acta Astronautica, 32:749–755, 1994.
7. Mewaldt, R. A. Cosmic Rays, available online at http://www.srl.caltech.edu/personnel/dick/cos_encyc.html, 1996.
8. Dachev, Ts., Horneck, G., Häder, D.-P., Lebert, M., Richter, P., Schuster, M., Demets, R. Time profile of cosmic radiation exposure during the EXPOSE-emission: the R3D instrument. Journal of Astrobiology 12 (5), 403–411, 2012, http://eea.spaceflight.esa.int/attachments/spacestations/ID501800a9c26c2.pdf.
9. Vette, J. I. The NASA/National Space Science Data Center Trapped Radiation Environment Model Program (1964–1991). NSSDC/WDCA-R&S, pp. 91–92, 1991.
10. Dachev, T. P., Semkova, J., Tomov, B., Matviichuk, Yu., Dimitrov, Pl., Koleva, R., Malchev, St., Reitz, G., Horneck, G., De Angelis, G., Häder, D.-P., Petrov, V., Shurshakov, V., Benghin, V., Chernykh, I., Drobyshev, S., and Bankov. N. G. 2011. Space shuttle drops down the SAA doses on ISS. Adv Space Res. 11:2030–2038, http://dx.doi.org/10.1016/j.asr.2011.01.034.
11. Heynderickx, D., Lemaire, J. and Daly, E. J. 1996, Historical review of the different procedures used to compute the L-Parameter. Radiation Measurements. 26, 325-331, 1996.
12. Dachev, T. P., B. T. Tomov, Yu. N. Matviichuk, Pl. G. Dimitrov, N. G. Bankov, G. Horneck; D.-P. Häder. Overview of the ISS radiation environment observed during EXPOSE-R2 mission in 2014-2016, Space weather, 2017. (Submitted)
13. Cliver, E. W., and Cane H. V. The last word: gradual and impulsive solar energetic particle events. Eos, Trans. AGU, 83, 61, 2002.
14. Mertens, C. J., Wilson, J. W., Blattnig, S. R., Solomon, S. C., Wiltberger, M. J., Kunches, J., Kress, B. T., Murray, J. J. Space Weather Nowcasting of Atmospheric Ionizing Radiation for Aviation Safety. NASA Langley Research Center 2007. Available online at: http://ntrs.nasa.gov/archive/nasa/casi.ntrs.nasa.gov/20070005803_2007005368.pdf, December 2013.
15. Lantos, P. 1993. The Sun and its effects on the terrestrial environment. Radiation Protection Dosimetry 48 (1), 27–32, 1993.
16. Häder, D.-P., Richter, P., Schuster, M., Dachev, Ts., Tomov, B., Dimitrov, P., Matviichuk, Yu. R3D-B2—Measurement of ionizing and solar radiation in open space in the BIOPAN 5 facility outside the Foton M2 satellite. Advances in Space Research, 43, 1200–1211, 2009, http://dx.doi.org/10.1016/j.asr.2009.01.021.
17. Dachev, Ts. P., Tomov, B. T., Matviichuk, Yu. N., Dimitrov, P. G., Bankov, N. G. Relativistic electrons high doses at international space station and Foton M2/M3 satellites. Adv. Space Res., 44 1433–1440, 2009, http://dx.doi.org/10.1016/j.asr.2009.09.023.
18. Damasso, M., Dachev Ts., Falzetta G., Giardi M. T., Rea G., Zanini A. The radiation environment observed by Liulin-Photo and R3D-B3 spectrum-dosimeters inside and outside Foton-M3 spacecraft, Radiation Measurements, V. 44, N0 3, 263-272, doi:10.1016/j.radmeas.2009.03.007, 2009.
19. Reitz, G., R. Beaujean, E. Benton, S. Burmeister, T. Dachev, S. Deme, M. Luszik-Bhadra, P. Olko Space radiation measurements on-board ISS-The DOSMAP experiment, Radiat. Prot. Dosim. 116 (1-4), 374-379, 2005.
20. Slaba, T. C., Blattnig S. R., Badavi F. F., Stoffle N. N., Rutledge R. DLee., K. T., Zapp E. N., Dachev T. P. and Tomov B.T. Statistical Validation of HZETRN as a Function of Vertical Cutoff Rigidity using ISS Measurements. Adv. Space Res., 47, 600-610, doi:10.1016/j.asr.2010.10.021, 2011.
21. Nealy, J. E., Cucinotta, F. A., Wilson, J. W., Badavi, F. F., Zapp, N., Dachev, T., Tomov, B. T., Semones, E., Walker, S. A., Angelis, G. De, Blattnig, S. R., Atwell, W., 2007. Pre-engineering spaceflight validation of environmental models and the 2005 HZETRN simulation code. Advances in Space Research 40 (11), 1593–1610, 2007, http://dx.doi.org/10.1016/j.asr.2006.12.030.
22. Badavi, F.F., 2014. Validation of the New Trapped Environment AE9/AP9/SPM at Low Earth Orbit, Advances in Space Research, 54, 917-928. http://dx.doi.org/10.1016/j.asr.2014.05.010.
23. Dachev, Ts., G. Horneck, D.-P. Häder, M. Schuster, and M. Lebert. EXPOSE-R cosmic radiation time profile, Journal of Astrobilogy, 14, 17-25, 2015. http://dx.doi.org/10.1017/S1473550414000093
24. Dachev, T. P., B.T. Tomov, Yu. N. Matviichuk, Pl. G. Dimitrov, N. G. Bankov, V. V. Shurshakov, O. A. Ivanova, D.-P. Häder, M.T. Schuster, G. Reitz, G. Horneck. “BION-M” №1 spacecraft radiation environment as

observed by the RD3-B3 radiometer-dosimeter in April-May 2013, Journal of Atmospheric and Solar-Terrestrial Physics. 123, 82-91, 2015. http://dx.doi.org/10.1016/j.jastp.2014.12.011

25. Spurny, F., T. Dachev, On Board Aircrew Dosimetry with a Semiconductor Spectrometer, Radiat. Prot. Dosim. 100, pp 525-528, 2002, http://rpd.oxfordjournals.org/cgi/content/abstract/100/1-4/525.
26. Dachev, Ts., Tomov, B., Matviichuk, Yu., Dimitrov Pl., Lemaire, J., Gregoire, Gh., Cyamukungu, M., Schmitz, H., Fujitaka, K., Uchihori, Y., Kitamura, H., Reitz, G., Beaujean, R., Petrov, V., Shurshakov V., Benghin, V. Spurny, F. Calibration results obtained with Liulin-4 type dosimeters, Adv. Space Res. 30, 917-925, doi:10.1016/S0273-1177(02)00411-8, 2002.
27. Uchihori, Y., H. Kitamura, K. Fujitaka, Ts. P. Dachev, B. T. Tomov, P. G. Dimitrov, Y. Matviichuk. Analysis of the calibration results obtained with Liulin-4J spectrometer-dosimeter on protons and heavy ions, Radiation Measurements, 35, 127-134, 2002. doi:10.1016/S1350-4487(01)00286-4
28. Dachev, Ts. P. Characterization of near Earth radiation environment by Liulin type instruments, Adv. Space Res., 1441-1449, doi:10.1016/j.asr.2009.08.007, 2009.
29. Berger, M. J., Coursey, J. S., Zucker, M. A., Chang, J. Stopping-power and range tables for electrons, protons, and helium ions. NIST Standard Reference Database 124, Available online at: http://www.nist.gov/pml/data/star/index.cfm, October, 2013.
30. Zheng, Y., Lui, A. T. Y., Li, X., Fok, M.-C., 2006. Characteristics of 2–6 MeV electrons in the slot region and inner radiation belt. J. Geophys. Res. 111, A10204, 2006.
31. Haffner, J. Nuclear radiation and safety in space. M, Atomizdat, pp 115, 1971. (in Russian).
32. Forbush, S. E., World-wide cosmic ray variations, 1937–1952. Journal of Geophysical Research, 59(4), 525-542 1954.
33. Filz, R. & E. Holeman, Time and altitude dependence of 55-MeV trapped protons, August 1961 to June 1964. J. Geophys. Res. 70(23), 5807-5822, 1965.
34. Dachev, T. P., Profile of the ionizing radiation exposure between the Earth surface and free space, Journal of Atmospheric and Solar-Terrestrial Physics, 102, September 2013, 148–156, 2013, http://dx.doi.org/10.1016/j.jastp.2013.05.015.
35. Benghin, V. V., Petrov, V. M., Panasyuk, M. I., Volkov, A. N., Lyagushin, V. I., Nikolaev, I. V., Nechaev, O. Yu., Tel'tsov, M. V., Lichnevskii, A. E., 2010. Nine years of the radiation monitoring system operating in service module of ISS. Fifteenth WRMISS Workshop, Frascati, Italy, 7–9 September 2010. Available online at: http://wrmiss.org/workshops/fifteenth/Benghin.pdf , December 2013.
36. Gaza, R., Zhou, D., Roed,Y., Steenburgh,R., Lee,K., Flanders,J., Fry, D., Semones, E., Reitz, G., Berger, T., O'Sullivan, D., Zapp, N., 2010. ISS Measurements at Solar Minimum (2008–2010). Available online at http://wrmiss.org/workshops/fifteenth/Zapp.pdf.